

# The Use of the Wind Tunnel in Connection With Aircraft-Design Problems

BY TH. VON KÁRMÁN<sup>1</sup> AND CLARK B. MILLIKAN,<sup>2</sup> PASADENA, CALIF.



T. VON KÁRMÁN

The paper is divided into two parts, the first of which deals with the general problem of extrapolating wind-tunnel results to full-scale free-flight conditions in connection with the initial prediction of overall performance characteristics of airplanes. Using the notation of Oswald, it is found that the three parameters about which the designer would like information from the wind tunnel are: the "airplane efficiency factor" giving the variation in parasite drag with lift coefficient, the "equivalent parasite area" giving essentially the minimum parasite drag, and the maximum lift coefficient. If the tests are made at Reynolds' numbers of the order of 1,500,000 or larger and on models of modern "clean" airplanes, the extrapolation of the first parameter to full scale is felt to be trustworthy



C. B. MILLIKAN

for gliding flight. The need for further data on the influence of the change to power-on flight is mentioned. For the second parameter the effect of the change in Reynolds' number involved in the extrapolation is shown to be important, and a method for carrying out the extrapolation is described. This method is based on the modern hydrodynamical theory of skin friction, and has already met with some success as developed and used at the Guggenheim Aeronautics Laboratory of the California Institute of Technology. In connection with the third parameter, it is shown that the influence of Reynolds' number and turbulence on the value of the maximum-lift coefficient is very large. The importance and confusion attending this phenomenon led some time ago to its intensive investigation at the laboratory. The more important results of an experimental and a theoretical approach to the problem are discussed. The experimental researches involved the testing of a 6-ft-span N.A.C.A. 2412 airfoil at a series of Reynolds' numbers and with various degrees of turbulence produced artificially in the wind tunnel through the introduction of grids or screens upstream from the model. The results furnish quantitative evi-

dence of the considerable dependence of  $C_{Lmax}$  on Reynolds' number and turbulence, and in particular demonstrate the fact that, even at fairly large Reynolds' numbers, the value of  $C_{Lmax}$  may be increased by as much as 30 per cent by introducing artificial turbulence into a normally very smooth wind-tunnel flow. The theoretical investigation involves an analysis of the boundary-layer flow around an N.A.C.A. 2412 airfoil, and is particularly concerned with the transition from the laminar to the turbulent regime and with the separation of the laminar boundary layer from the upper surface of the airfoil. The second part of the paper gives illustrations of the diverse nature of the special aircraft-design problems for which the wind tunnel may give valuable information. The examples discussed are all chosen from investigations initially undertaken at our laboratory at the request of aircraft manufacturers and at their expense. Many of the problems so begun developed an independent scientific interest, so that the tests were subsequently amplified by the staff to a degree not at all contemplated when the work was started. A series of six distinct types of investigations is included in the samples considered.

## INTRODUCTION

IT IS ABOUT 25 years since systematic tests on stationary models in artificially created air streams were first used as an aid to the design and performance prediction of airplanes. Widely varying opinions as to the practical applicability of this type of measurement have been held by aeronautical engineers. The naive idea that the results of such measurements could be applied without corrections to full-scale conditions was very early

abandoned. The corrections due to the finite dimensions of the wind stream have been found comparatively easily by the application of aerodynamic theory. The establishment of model rules to take into account the effect of scale in size and velocity, i.e., Reynolds' number, has proved to be much more difficult. The opinion has been widely expressed that full information could be obtained only by carrying out the model tests at full-scale Reynolds' number. It is well known that the so-called variable-

<sup>1</sup> Director of Guggenheim Aeronautics Laboratory, California Institute of Technology. Mem. A.S.M.E. Dr.-Ing. von Kármán received his M.E. at Budapest in 1902 and Ph.D. at Göttingen in 1908; honorary degree of Doctor of Engineering, University of Berlin, 1929. He was Privat-Docent, Göttingen, 1910-1913; Professor of Mechanics and Aerodynamics, Director of the Aerodynamical Institute, University of Aachen, 1913; member of Gesellschaft der Wissenschaften zu Göttingen, 1925; foreign member of the Royal Academy of Sciences, Turin, 1928; Director of the Graduate School of Aeronautics, California Institute of Technology, 1928.

<sup>2</sup> Assistant Professor of Aeronautics, Daniel Guggenheim Graduate School of Aeronautics, California Institute of Technology. Assoc-

Mem. A.S.M.E. Professor Millikan was born in Chicago in 1903, and received his Ph.B. from Yale University in 1924 and Ph.D. in Physics and Mathematics from California Institute of Technology in 1928. He was a Teaching Fellow at the California Institute of Technology from 1924 to 1928, and since then has held his present position.

Contributed by the Aeronautics Division and presented at the Semi-Annual Meeting, Chicago, Ill., June 26 to July 1, 1933, of THE AMERICAN SOCIETY OF MECHANICAL ENGINEERS.

NOTE: Statements and opinions advanced in papers are to be understood as individual expressions of their authors, and not those of the Society.

density wind tunnels and the N.A.C.A. giant tunnel have been built for this purpose. Both of these types of wind tunnel have already made very valuable contributions to the development of experimental aerodynamics, but there are certain difficulties connected with each. The relatively small size of the models used in the variable-density tunnel makes the reproduction of small details rather difficult. Also, the initial cost of such wind tunnels is so large as to almost rule out their use by other than governmentally supported institutions. The latter remark applies *a fortiori* to the giant tunnel, and furthermore, the cost of models and of operations is very large. A further complication is introduced by the fact that measurements carried out at the same Reynolds number may lead to very different results if the internal structure of the artificial air streams (i.e., their state of turbulence) is different. In view of this situation, the authors believe that it is very important to analyze the conditions under which measurements in a medium-sized wind tunnel can be applied reliably to full-scale conditions. Obviously, it is necessary that the measurements be carried out at a Reynolds number above those producing critical changes in the flow and in a range where certain theoretical extrapolations connected with friction can be safely made. It is also desirable that the wind stream for the tests be as free from turbulence as possible, since it is very simple to introduce artificial turbulence, but extremely difficult to remove an already existing turbulence. The wind tunnel of the Guggenheim Aeronautics Laboratory of the California Institute of Technology has been built in such a way as

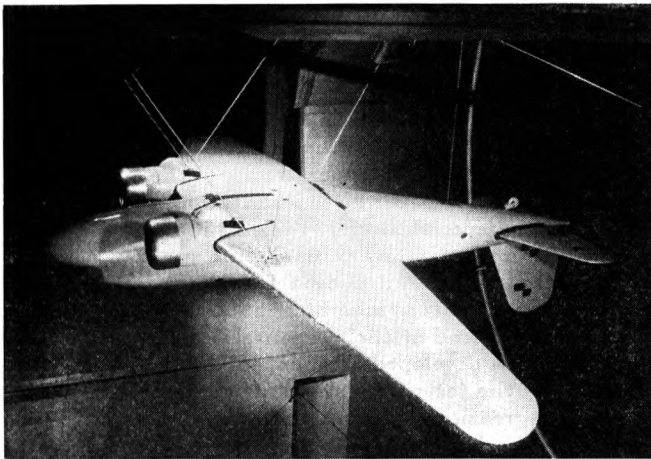


FIG. 1 MODEL SUSPENDED (INVERTED) IN THE GUGGENHEIM AERONAUTICS LABORATORY WIND TUNNEL READY FOR TESTS  
(The model span is 7 $\frac{3}{4}$  ft.)

to satisfy these conditions as fully as possible. The first part of this paper is devoted to a discussion of the applicability of the measurements made in such a wind tunnel, with particular reference to performance predictions. The second part discusses a series of investigations collected in order to show the wide range in the type of design problems which can be attacked using this type of wind tunnel.

A detailed description of the wind tunnel has previously been published,<sup>3</sup> so that only the chief characteristics will be repeated here. The diameter of the closed working section is 10 ft, and the wind speed for normal operation is 200 mph. The airplane models tested have, in general, spans of between 5 and 8 ft, so that the usual Reynolds number based on the wing chord lies

<sup>3</sup> C. B. Millikan and A. L. Klein, "Description and Calibration of 10-Foot Wind Tunnel at California Institute of Technology," presented at the Pacific Coast Aeronautics Meeting, Berkeley, Calif., June 9 to 10, 1932 (mimeographed).

between 1,500,000 and 2,000,000. The suspension system has been very carefully designed to eliminate interference between the model and its supports to as large an extent as possible. A photograph of a typical model mounted in the wind tunnel and ready for testing is given in Fig. 1. All of the experimental data discussed in this paper were obtained in this wind tunnel. Unless otherwise specified, the notation employed is that defined by the N.A.C.A. as the standard American notation using absolute coefficients.

A considerable group of graduate students under the direct supervision of Drs. A. L. Klein and C. B. Millikan has carried out the wind-tunnel investigations discussed in this paper. In particular, acknowledgment should be made of the contributions of Messrs. W. B. Oswald, W. H. Bowen, N. B. Moore, and R. Mills. The design of the wind-tunnel balances, rigging, and all auxiliary apparatus has been done by Dr. Klein.

## I—INITIAL PERFORMANCE PREDICTION

The modern methods of performance estimation which have recently been published here and abroad substitute for a graphical method of calculation an analytical one using certain definite design parameters of the airplane to which numerical values are assigned. The problem of the airplane designer is to determine these numerical values as accurately as possible. At our laboratory the most accurate, rapid, and satisfactory method of performance prediction has been found to be the analytical one developed by Oswald and presented in full in N.A.C.A. Technical Report No. 408.<sup>4</sup> The design parameters used in this method are: the gross weight  $W$ , the design thrust horsepower  $thp_m$ , the wing area  $S$ , the effective span  $b$ , the equivalent parasite area  $f$ , and the maximum-lift coefficient  $C_{Lmax}$ . Of these, the weight and wing area are known for any proposed design. The design thrust horsepower is the product of the design brake horsepower and the design propulsive efficiency. The first is given by the engine, and the second may now be very satisfactorily estimated for any normal engine and cowling arrangement as a result of the very beautiful and complete investigations carried out in its propeller research wind tunnel by the N.A.C.A. The effective span may be expressed by the relation  $b_e^2 = e(kb)^2$ , where  $e$  is the so-called airplane efficiency factor,  $b$  is the largest span of the airplane, and  $k$  is Munk's span factor;  $b$  is given, and  $k$  may readily be calculated from the geometry of the wing cellule. Hence, the three parameters for which the designer must obtain values are  $e$ ,  $k$ , and  $C_{Lmax}$ . In the remainder of this section the methods for estimating the full-scale values of these parameters which have been used at the laboratory are described.

### 1 EFFICIENCY FACTOR $e$

A polar of  $C_D$  versus  $C_L$  is plotted from the wind-tunnel measurements corrected for tare drag and wind-tunnel wall interference. The parasite-drag coefficient  $C_{Dp}$  is defined as

$$C_{Dp} = C_D - C_{Di} = C_D - \frac{C_L^2}{\pi b_e^2 / S}$$

An induced-drag parabola ( $C_{Di}$  versus  $C_L$ ) is now plotted on the same sheet as the original polar, in such a manner that the difference in abscissas ( $C_{Dp}$ ) between it and the original polar is as nearly constant as possible over the range of  $C_L$ 's included in the normal flying range below the stall. This is assumed to be the corrected induced-drag polar for the airplane in Oswald's sense; i.e., it is the curve corresponding to

<sup>4</sup> W. B. Oswald, "General Formulas and Charts for the Calculation of Airplane Performance," N.A.C.A. Technical Report No. 408 (1932).

$$C_{Di} = \frac{C_L^2}{\pi b e^2 / S}$$

From this polar  $b_e^2 S$  is determined, and, since  $S$ ,  $b$ , and  $k$  are known, the value of  $e$  is easily deduced. This value of  $e$  is assumed to be the same as that for the full-sized airplane in free flight.

The assumptions which are made in this extrapolation are that the influences of the following changes in passing from model to full scale are unimportant:

- (a) Changes in shape especially in small details
- (b) Change in Reynolds' number
- (c) Change in character of air flow (turbulence)
- (d) Change from power off to power on.

The validity of (a) depends upon the accuracy of the model work, the size of the model, and the cleanness or complication of the external design of the airplane. All three of these points are interrelated. For a very complicated design with many wires, struts, fittings, and excrescences, it is almost impossible to duplicate the airplane accurately enough in any model much smaller than one to be tested in the N.A.C.A.'s full-scale wind tunnel. For modern high-speed designs, with cantilever or simply braced wings, retractable or completely faired landing gears, enclosed cockpits, etc., it is our belief that models of sufficient accuracy can fairly readily be constructed with spans of the order of 6 to 8 ft. With regard to (b), there is no evidence with which the authors are familiar to indicate that there is any important change with Reynolds' number in the variation of  $C_{D_p}$  with  $C_L$ , at least above Reynolds' numbers (based on wing chord) of the order of 1,000,000. The same state of affairs holds for (c) as for (b). With respect to (d), recent flight test researches, especially those carried out by the D.V.L. in Germany, indicate that in certain cases there is a very considerable change in  $e$  in passing from gliding to power-on flight. Hence predictions of  $e$  made in the manner here suggested are strictly valid only for gliding flight, but are believed to furnish valuable indications, at least for power-on flight. Experiments are now in hand at the Guggenheim Aeronautics Laboratory here, using small motors mounted in the wind-tunnel models and driving small propellers during the experiments, which it is hoped will give sufficient data to enable the extension of accurate predictions of  $e$  to the case of power-on flight.

2 EQUIVALENT PARASITE AREA  $f$

Having determined the parasite-drag coefficient by the method of the last section,  $f$  for the full-scale airplane is most naively obtained from the formula (defining  $f$ ):

$$f = C_{D_p} S \dots \dots \dots [1]$$

where  $S$  is the wing area of the full-size airplane. Such an extrapolation involves the same assumptions (a) to (d) as were discussed in the preceding section; (a) has already been considered; and any question as to (d) is eliminated if propulsive efficiencies are taken from the N.A.C.A.'s reports previously referred to, in which propulsive efficiencies are so defined as to take into account the effects of changes from power off to power on. With respect to (c), turbulence can exert an influence on  $C_{D_p}$  in two different ways: eddy resistance depends on the location of separation points, which may change with the turbulence conditions; skin friction is influenced by the transition between the laminar and turbulent régimes in the boundary layer. Both influences can be eliminated if the models tested are clean enough and the tests are carried out at such high Reynolds' numbers that critical points do not occur near the high-speed attitude of the plane and the boundary layer is turbulent over the major part of the

model surface. It appears that these conditions are satisfied for models of modern high-speed airplanes tested at Reynolds' numbers above 1,000,000 or 1,500,000. There remains (b), the effect of the change in Reynolds' number or the scale effect proper. For modern high-speed transport planes a considerable extrapolation is here necessary, even for tests carried out in the N.A.-C.A.'s variable-density or full-scale wind tunnels, since for such planes at maximum speed the Reynolds number based on wing chord may reach values of the order of 20,000,000 to 30,000,000. The following method of making this extrapolation has recently been devised by the junior author and used with some success.

Parasite drag may be divided into two categories: eddy resistance or form drag, which is approximately independent of Reynolds' number (assuming that no critical points occur in the range considered), and skin friction. If the scale of the tests is sufficiently large, as previously indicated ( $R \sim 1,000,000$  to 1,500,000), the boundary layer may be assumed to be turbulent over practically all of the model, so that the friction may be considered as purely turbulent skin friction. The theory of turbulent skin friction has been actively investigated in the last decade. It was for some time accepted that the coefficient of skin friction for smooth, flat surfaces was proportional to the  $1/5$  power of the Reynolds number, so that it appeared at one time as if this "power law" represented a basic physical law.

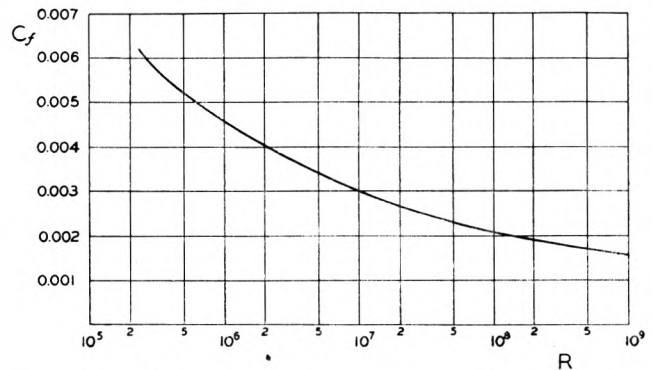


FIG. 2 COEFFICIENT OF SKIN FRICTION  $C_f$  AS FUNCTION OF THE REYNOLDS NUMBER  $R$ , FOR SMOOTH FLAT PLATES (From Von Kármán's theory.)

This belief was subsequently proved to be false when further experimental data obtained at higher Reynolds' numbers than had previously been investigated showed that as  $R$  increased, the exponent decreased from  $1/5$  to  $1/6$ , then to  $1/7$ , and so on. These discoveries left the basic theory of turbulent skin friction in a very troubled and unhappy state. Finally, the senior author, using reasoning based on considerations of dynamical similarity, was able to show that a general law could be formulated giving a logarithmic formula for the variation of the coefficient of skin friction with Reynolds' number.<sup>5</sup> The earlier power laws were shown to be essentially interpolation formulas for this general law, which has since been verified experimentally up to the highest Reynolds' numbers yet attainable. According to this theory, the formula connecting the coefficient of the skin friction and Reynolds' number can be written<sup>6</sup>

$$\frac{0.242}{\sqrt{(C_f)}} = \log_{10} (RC_f)$$

<sup>5</sup> Th. von Kármán, "Mechanische Aehnlichkeit und Turbulenz," *Göttingen Nachrichten* (Math.-Phys. Klasse), 1930; see also Proceedings of the Third International Congress for Applied Mechanics, Stockholm (1930), vol. I, p. 85.

<sup>6</sup> Th. von Kármán, "Quelques Problèmes Actuels de L'Aérodynamique," *Journées Techniques Internationales de L'Aéronautique*, Paris, 1932.



The values of  $C_f$  and  $R$  are represented in Fig. 2.  $C_f$  is strictly the skin friction on a flat plate parallel to the flow and is defined as the average frictional force per unit "wetted area" on a flat plate of length  $l$  in the direction of flow divided by the dynamic pressure.  $R$  is defined in terms of the free-stream velocity and the length  $l$ .

In applying the results of this theory to the problem under consideration, two extreme cases are considered:

- Case 1: Only the wing-profile drag is considered as turbulent skin friction; the remaining parasite drag is assumed to be form drag and as such is independent of Reynolds' number
- Case 2: The entire parasite drag is assumed to be skin friction. The characteristic length  $l$  is taken as the mean wing chord.

Considering case 1, and letting  $( )_m$  correspond to model conditions and  $( )_f$  correspond to full scale, while  $C_{D_o}$  denotes wing-profile drag and  $R$  the Reynolds number, we have

$$\frac{C_{D_{of}}}{C_{D_{om}}} = \frac{C_f(R_f)}{C_f(R_m)} \dots \dots \dots [2]$$

where the length in  $R$  is taken as the mean wing chord, and  $C_f$  is read from Fig. 2. From the  $C_{D_{of}}$  determined in this way,  $f_{wings}$  is calculated from Equation [1]. The equivalent parasite area for the remainder of the airplane is calculated in the same way, assuming the drag coefficient to be independent of  $R$ . The total  $f$  for full-scale conditions is then the sum of these two parasite areas. For case 2, the procedure is the same except that

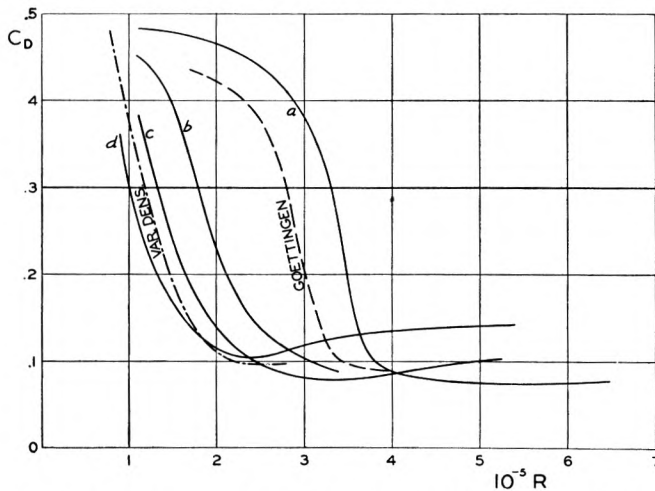


FIG. 3 SPHERE-DRAG COEFFICIENT  $C_D$ , VERSUS REYNOLDS' NUMBER  $R$ , FOR VARIOUS WIND STREAMS

(Curves  $a$ ,  $b$ ,  $c$ , and  $d$  refer to the wind tunnel of the Guggenheim Aeronautics Laboratory of the California Institute of Technology, with no grid and with grid 48 in., 20 1/2 in., and 10 1/2 in. upstream from the model, respectively. The curves for the N.A.C.A. variable-density and the Göttingen wind tunnels are also included.)

in Equation [2] the profile-drag coefficient is replaced by the total parasite-drag coefficient  $C_{D_p}$ , and there is no additional term with constant-drag coefficient. Case 1 should give too large a full-scale  $f$  and case 2 somewhat too small a value. The actual  $f$  should be between the two, its proximity to one or the other being estimated on the basis of the amount of form drag to be expected—i.e., on the cleanness of the airplane design. As an example, the following data are given, derived from tests on a model of an observation-type military monoplane with wire bracing, pylon above the wing, tripod landing gear with wheel fairings, and open cockpit. The maximum velocity  $V_m$  was cal-

culated from  $f$ , using the methods of Oswald's paper (loc.cit.):

Model results scaled up without Reynolds' number correction:  $V_m = 180$  mph.

Wing-profile drag only corrected to full scale:  $V_m = 186$  mph.

Total parasite drag considered as skin friction and corrected to full scale:  $V_m = 205$  mph.

Flight tests on the actual airplane gave  $V_m = 195$  mph—i.e., almost exactly half-way between the two extrapolations. This airplane was not especially clean in comparison with modern transport planes, the total parasite drag being about four times as large as the wing-profile drag. For some recent planes the total parasite drag is only about twice the wing-profile drag, and in such cases the two extrapolations would give results much less far apart, with the actual  $V_m$  lying nearer to the higher estimate because of the smaller percentage of form drag.

3 MAXIMUM LIFT COEFFICIENT  $C_{L_{max}}$

In extrapolating wind-tunnel results for  $C_{L_{max}}$  to full scale in order to estimate landing speeds, the same changes (a) to (d) previously discussed must again be considered. Item (d) may be neglected, since in practise the landings are almost always made with the motor idling, although there is evidence that in some cases of unfortunate placing of the propeller relative to the wing the presence of an idling or stopped propeller lowers  $C_{L_{max}}$  to some extent. With regard to (a), investigations here at the Guggenheim Aeronautics Laboratory and elsewhere have shown that slight roughness or protuberances near the leading edge of a wing may lower its  $C_{L_{max}}$  very appreciably. Hence the finish of this portion of the model should be as perfect as possible. At the aeronautics laboratory here this is accomplished by spraying the model with several coats of lacquer and rubbing down to a high polish. In some cases of rather protracted or interrupted tests this process has been repeated several times during the course of an investigation. By this means highly reproducible values of  $C_{L_{max}}$  are attained which are thought to permit safe extrapolation to full scale, at least in so far as (a) is concerned. The effects of (b) and (c) (i.e., Reynolds' number and turbulence) are very large and have in the past been very confusing, as is evidenced by the large discrepancies between the values of  $C_{L_{max}}$  reported by different wind tunnels for the same airfoil section. The confusion in this matter prompted Drs. Klein and Millikan to undertake an elaborate experimental investigation of the phenomenon in the spring of 1932, introducing turbulence artificially into the wind-tunnel stream by means of screens placed upstream from the model. Shortly afterward the present authors began work on a theoretical discussion of the problem, which turned out to be correspondingly elaborate. The complete results of both researches are appearing currently in technical journals. In the remaining paragraphs of this section a brief account of the most important results will be given.<sup>7</sup> The experiments were carried out on a model of the N.A.C.A. 2412 section with rectangular plan form, aspect ratio 6, and span 6 ft. The model was furnished by the Boeing Airplane Company and was very accurately made of laminated wood finished to a high polish. For the results to be discussed here, turbulence was introduced into the wind stream by placing a grid of rods 1/8 in. in diameter, spaced 3/4 in. apart, at various distances upstream from the model. The rods were perpendicular to the wind stream and to the span of the model, and the grid was of such a size and so placed that the entire wing was in its "wind shadow" at all angles of attack. For each position of the grid, measurements were taken of the resistance of a sphere placed in the position normally occupied by the center

<sup>7</sup> See also Th. von Kármán, "Quelques Problèmes Actuels de l'Aérodynamique," Journées Techniques Internationales de l'Aéronautique, Paris, 1932.



of the wing. Using the criterion suggested by Dryden and Kuethe,<sup>8</sup> the values of the Reynolds number at which the sphere-drag coefficient had the value 0.3 furnished a measure for the degree of turbulence caused by the grid in the different positions. The sphere-drag curves obtained for three positions of the grid and with the grid removed are given in Fig. 3. The curve re-

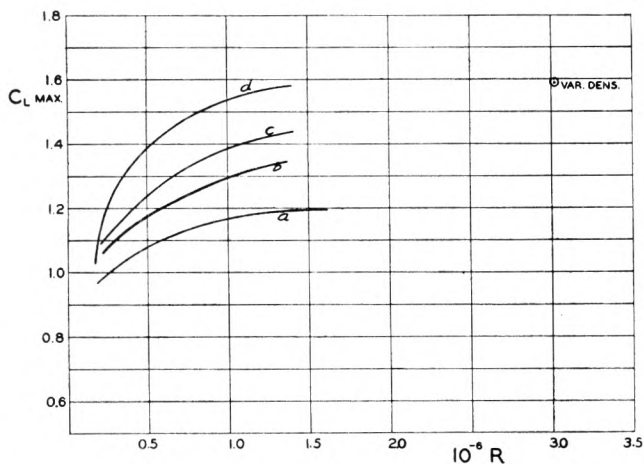


FIG. 4  $C_{Lmax}$  VERSUS  $R$  FOR N.A.C.A. 2412 AIRFOIL (CHORD = 12 IN.)

(The curves *a*, *b*, *c*, and *d* refer to the same flow conditions as to the corresponding curves of Fig. 3. The value reported from the variable-density tunnel is indicated.)

ported for the N.A.C.A. variable-density tunnel is also included for comparison.<sup>9</sup> It will be noticed that the degree of turbulence in the variable-density tunnel is apparently about midway between those obtained in the laboratory tunnel with the grid in the two positions nearest the model (*c* and *d*). The variable-density tunnel is chosen for the comparison, since one of the main purposes of the investigation was originally an attempt to explain the extremely large discrepancy between the values of  $C_{Lmax}$  for the 2412 wing reported from the variable-density tunnel and those obtained in our laboratory experiments.

For each of the configurations *a*, *b*, *c*, and *d*, polars were observed for the wing at a series of seven or eight Reynolds' numbers. Curves giving the result as regards  $C_{Lmax}$  are plotted in Fig. 4, together with a point giving the  $C_{Lmax}$  reported by the variable-density tunnel.<sup>10</sup> A curve midway between *c* and *d* extrapolated to  $R = 3,000,000$  would apparently come very close to the latter point. This result is entirely consistent with the sphere-drag curves of Fig. 3.

The conclusion to be drawn from these results is that both Reynolds' number and turbulence have very pronounced effects on  $C_{Lmax}$ . The variation with  $R$  is the more pleasant of the two, since it appears that at  $R \sim 1,500,000$  the curves are rapidly approaching horizontal asymptotes, so that extrapolation to higher values of  $R$  should be possible with some measure of confidence. This seems to be especially true for the curve *a* corresponding to the clean tunnel or the normal operating state. The variation with turbulence at once raises the question as to the degree of turbulence to be expected in free flight. Experiments are under way to determine the critical Reynolds' number

of a sphere mounted on an airplane flown under various conditions. It is hoped that these tests will furnish data pertinent to this question.

The theoretical investigation mentioned was undertaken in the hope that the physical mechanism underlying the results just described might be elucidated. The experimental fact was known that, even in the case that the general flow outside of a boundary layer is turbulent, the boundary layer starting from the stagnation point has a laminar character. However, the degree of the outside turbulence has a large effect on the transition point between the laminar and turbulent state in the layer itself. It was therefore suspected that the large influence of external turbulence on  $C_{Lmax}$  might be connected with this phenomenon. In view of the complexity of the phenomena, it was not at all expected that theoretical curves duplicating those of Fig. 4 could be deduced, but it was hoped that results similar enough to the experimental ones might be predicted, so that the essential physical processes involved might be visualized. For this purpose an analysis of the laminar boundary layer about a two-dimensional airfoil was attempted. A new method of discussing boundary layers with external pressure gradients was developed, of which the only element which need be discussed here is the following: Instead of using the distance along the solid surface from some origin as one of the variables of the problem, it was

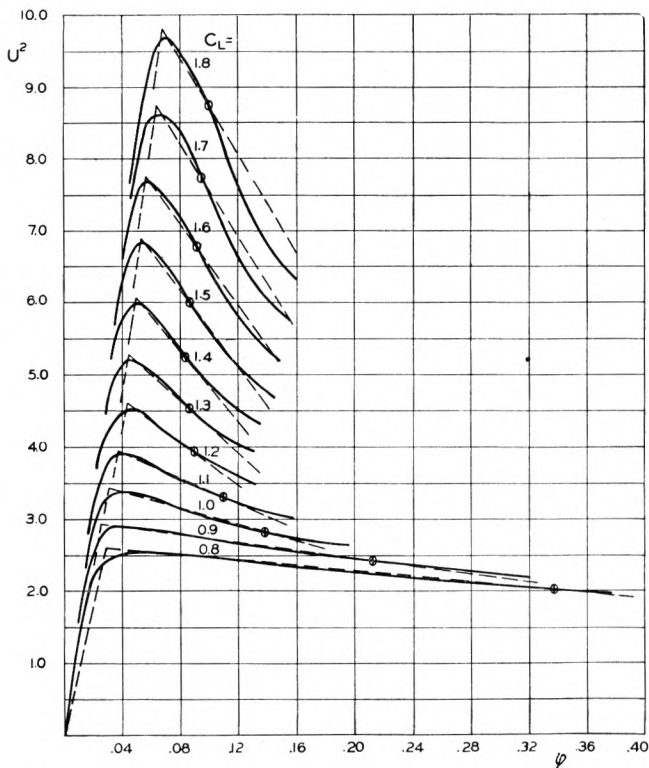


FIG. 5 COMPUTED VALUES OF  $U^2$  VERSUS  $\phi$  FOR N.A.C.A. 2412 AIRFOIL AT VARIOUS LIFT COEFFICIENTS

(The position of the separation point for each  $C_L$  is indicated by the oval crossing each curve. In order to make the figure clearer, the curves have not been extended to the origin. The dotted straight lines give the approximations to the theoretical curves which were used in the boundary-layer calculations.)

found convenient to use the value of the potential function  $\phi$  associated with the external potential flow measured from the forward stagnation point as origin. The value of  $\phi$  at any point is then merely of the line integral  $\int U ds$  along the surface from the stagnation point to the point in question, where  $U$  is the ratio of the potential velocity outside of the boundary layer to the

<sup>8</sup> H. L. Dryden and A. M. Kuethe, "Effect of Turbulence in Wind-Tunnel Measurements," N.A.C.A. Technical Report No. 342 (1930).

<sup>9</sup> John Stack, "Tests in the Variable-Density Wind Tunnel to Investigate the Effects of Scale and Turbulence on Airfoil Characteristics," N.A.C.A. Technical Note No. 364 (1931).

<sup>10</sup> E. N. Jacobs and K. E. Ward, "Tests of N.A.C.A. Airfoils in the Variable-Density Wind Tunnel, Series 24," N.A.C.A. Technical Note No. 404 (1932).

undisturbed flow velocity, and  $ds$  is an element of length along the airfoil surface, perpendicular to the span, divided by the airfoil chord.

The potential flow-velocity distribution over the upper surface of an N.A.C.A. 2412 airfoil from the stagnation point downstream was calculated by Theodorsen's method<sup>11</sup> for a series of values of  $C_L$ . The squares of the velocities so obtained are plotted against  $\varphi$  in Fig. 5. For simplicity in making the succeeding calculations, each of these curves was approximated by two intersecting straight lines, which are shown dotted in Fig. 5. The errors introduced by this approximation should be relatively unim-

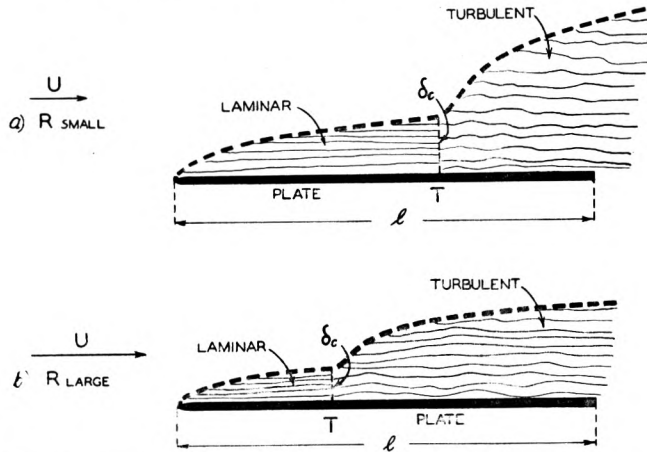


FIG. 6 SCHEMATIC DIAGRAM OF THE BOUNDARY LAYERS FOR FLOW ALONG A FLAT PLATE AT TWO REYNOLDS' NUMBERS ( $R = U1/\nu$ ) (The motion upstream of the transition point  $T$  as  $R$  increases is indicated.)

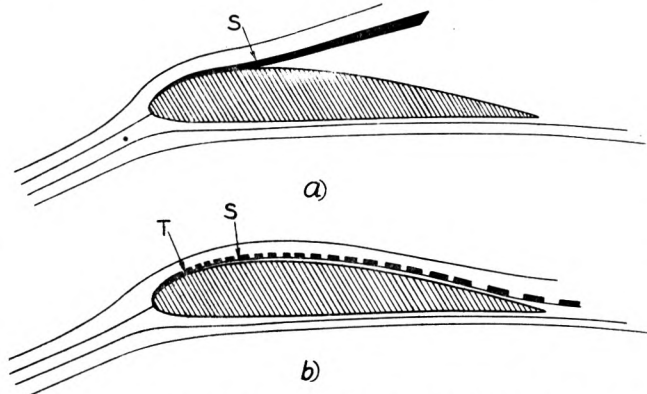


FIG. 7 DIAGRAM OF ALTERNATIVE FLOWS ABOUT AN AIRFOIL NEAR  $C_{Lmax}$

(The boundary layer over the upper surface is indicated by the heavy line. In (a) the transition point would be downstream from the separation point  $S$ , and the flow separates from the airfoil. In (b) the transition point  $T$  is upstream from the calculated separation point  $S$ , the turbulent layer (dotted) clings to the surface, and the separation does not occur.)

portant in view of the nature of the problem. The separation points at which the flow breaks away from the airfoil surface were calculated for the boundary layer associated with each of the curves, and are indicated on the figure. The boundary-layer thickness at the separation point  $\delta_s$  was determined for each of the curves, and a corresponding boundary-layer Reynolds' number  $R_{\delta_s}$  was defined by

$$R_{\delta_s} = \frac{U_s \delta_s}{\nu} \dots \dots \dots [3]$$

<sup>11</sup> Theodore Theodorsen, "Theory of Wing Sections of Arbitrary Shape," N.A.C.A. Technical Report No. 411 (1932).

where  $U_s$  is the potential velocity just outside the boundary layer and at the separation point and  $\nu$  is the coefficient of kinematic viscosity.

A result obtained both experimentally and theoretically for boundary layers along flat plates in a uniform flow was now extended to the boundary layers under consideration. This result is the following: If a boundary-layer Reynolds' number  $R_{\delta}$  be associated as in Equation [3] with the laminar boundary-layer thickness  $\delta$ , along a flat plate parallel to a uniform flow, then for any given degree of turbulence in the external flow there exists a definite critical value of  $R_{\delta}$ , called  $R_{\delta_c}$ , at which the laminar flow in the boundary layer becomes unstable. Hence, when  $R_{\delta}$  (which increases continuously as one goes downstream from the leading edge) reaches the value of  $R_{\delta_c}$ , a transition point occurs. Upstream from this transition point the flow in the boundary layer is laminar, while downstream the flow is turbulent (see Fig. 6).

The variation of  $\delta$  with the external velocity  $U$  is such that, as  $U$  (or the basic Reynolds' number  $R$  referred to the length of the plate) increases, the transition point moves upstream for a given  $R_{\delta_c}$ . The value of  $R_{\delta_c}$  depends on the degree of turbu-

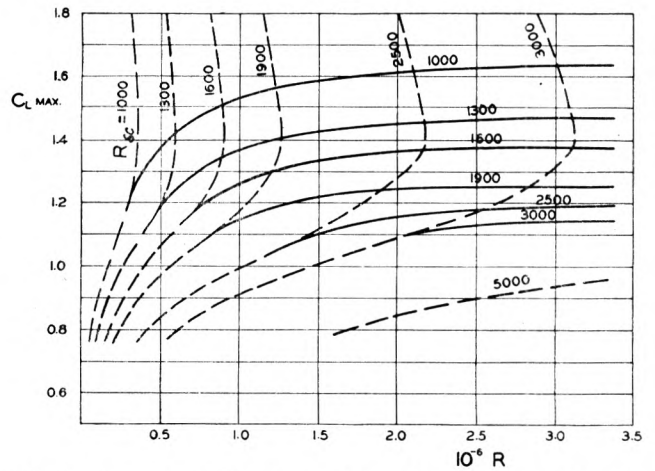


FIG. 8 THEORETICAL CURVES OF  $C_{Lmax}$  VERSUS  $R$  FOR VARIOUS VALUES OF  $R_{\delta_c}$

(Dotted curves represent calculated values. Solid curves represent rough extrapolations for the larger values of  $R$ , based upon reasoning given in the text.)

lence in the external flow in such a way that, as the turbulence increases,  $R_{\delta_c}$  decreases. For flow along a flat plate the values of  $R_{\delta_c}$  lie between about 10,000 for very smooth flows and about 1500 for very turbulent flows.

It was assumed that conditions are similar for the flow over an airfoil; i.e., for any external flow there exists an  $R_{\delta_c}$  such that when the boundary-layer Reynolds' number  $R_{\delta}$  reaches  $R_{\delta_c}$ , a transition point occurs and the boundary layer changes from laminar to turbulent. The problem under consideration can be put in the following way: Under what conditions can a certain value of  $C_L$  be reached? Obviously, it depends on which of  $R_{\delta_s}$  or  $R_{\delta_c}$  is the larger. If  $R_{\delta_s} < R_{\delta_c}$ , then the flow will separate from the airfoil at the calculated separation point, the assumed potential flow cannot exist, and the corresponding assumed value of  $C_L$  cannot be reached. If, on the other hand,  $R_{\delta_s} > R_{\delta_c}$ , the transition point will be upstream from the calculated separation point, and the flow at the latter point will no longer be laminar, as was assumed, but will instead be turbulent.

From experiments on spheres and other bodies, it is known that a turbulent boundary layer clings to a surface and resists separation to a much greater extent than does a laminar layer.

Therefore, in the case that  $R_{\delta_s} > R_{\delta_c}$ , the boundary layer will cling to the upper surface of the airfoil, and the possibility is given that the lift coefficient in question will be attained. The alternatives are illustrated schematically in Fig. 7. Whether the value of  $C_L$  in question will actually be reached depends on the behavior of the turbulent layer after the transition. Since very little is known about the laws governing the separation of turbulent boundary layers, it was assumed for this investigation that such a separation never occurs. Under this assumption,  $R_{\delta_s} = R_{\delta_c}$  is a limiting case such that the assumed  $C_L$  is just

general nature of the two families is very similar. For larger values of  $C_{Lmax}$  the theory gives very considerable effects of turbulence, but the shape of the theoretical curves is not satisfactory, for the reasons mentioned. The rather low values of  $R_{\delta_c}$  are not at all surprising when the unstable nature of the velocity profiles near a separation point is remembered. In any case the investigation shows without doubt that the physical basis of the large effect of the turbulence on the maximum-lift coefficient has been correctly determined as resting upon a transition-point versus separation-point contest. It will be noted that this is the same type of explanation as was given many years ago by Prandtl in connection with the then mysterious sphere-drag phenomenon.

II—SPECIAL DESIGN PROBLEMS

In this second part of the paper there will be discussed a series of different types of aircraft-design problems which have arisen and have been investigated in the wind tunnel of the Guggenheim Aeronautics Laboratory of the California Institute of Technology. Many of the tests to be considered originated at the request of commercial firms, in which cases the costs were borne by the firms concerned and the results were to remain confidential for a definite length of time. In such cases the illustrative data here furnished are of necessity incomplete.<sup>12</sup> In several in-

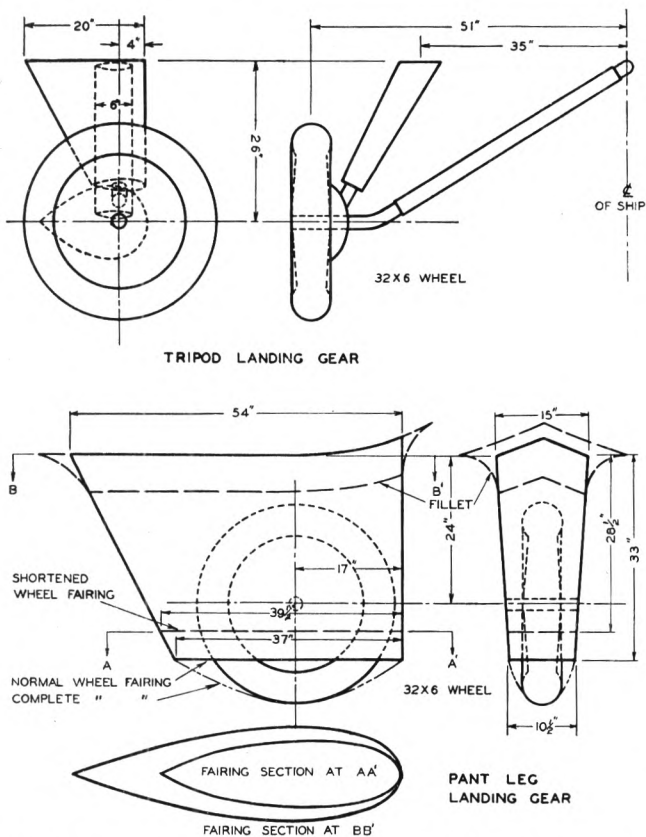


FIG. 9 TRIPOD AND "PANT LEG" LANDING GEARS OF NORTHROP ALPHA  
(Dimensions correspond to full scale. Model one-sixth full scale.)

attained. If the basic flow Reynolds' number  $R (= Ut/\nu$ , where  $t =$  airfoil chord) is decreased,  $R_{\delta_s}$  is decreased, separation occurs, and the assumed  $C_L$  is not attained. If  $R$  is increased, no separation occurs, and the assumed  $C_L$  is attained. Hence for every set of values of  $C_L$  and  $R_{\delta_c}$  we get certain definite values of  $R$  such that the assumed  $C_L$  is just the  $C_{Lmax}$  which can be obtained. Hence for a given  $R_{\delta_c}$  we may determine  $C_{Lmax}$  as a function of  $R$ . This has been done for a series of values of  $R_{\delta_c}$ , and the results are plotted as dotted curves in Fig. 8.

It will be observed that our assumption as to the lack of separation for turbulent boundary layers implies that unlimited values of  $C_{Lmax}$  are possible. This obviously represents an oversimplification, since somewhat analogous laws almost certainly govern the separation of turbulent and laminar boundary layers. Hence it is probable that those portions of the curves of Fig. 8 which are concave upward or have negative slopes are quite incorrect and should actually be replaced by branches similar to those drawn in solid lines.

If one compares the theoretical curves of Fig. 8 with the experimental ones of Fig. 4, one sees that for  $C_{Lmax} < 1.2$  to 1.4 the

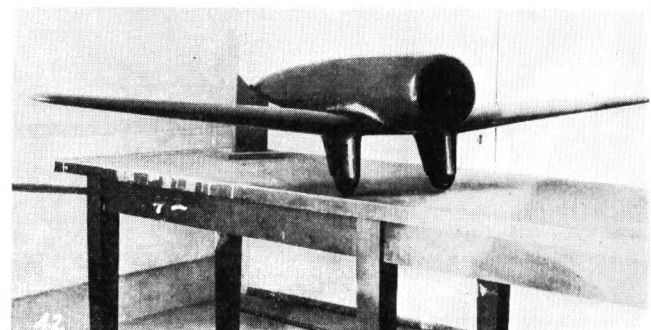


FIG. 10 PHOTOGRAPH OF NORTHROP ALPHA WIND-TUNNEL MODEL  
(With shortened "pant leg" landing gear.)

stances investigations begun in this manner developed a considerable scientific importance in the eyes of the laboratory staff, so that the tests were made much more extensive than had originally been contemplated, and arrangements were made for fairly early publication. The experiments discussed in Sections 2, 4, and 5 following belong in this latter category. The results to be presented here fall naturally into rather distinct groups, as indicated by the titles of the sections.

1 COMPARATIVE DRAG INVESTIGATIONS

The precision attained in ordinary drag measurements is limited essentially by the accuracy with which the tare drag can be determined. The precision of tare-drag measurements is considerably less than that for gross-drag observations, due chiefly to difficulties inherent to the tare-drag set-up and to unavoidable interference between the model and the supporting system. It is conservatively estimated that the tare drag is accurate to within about 5 per cent, which means that the minimum drag of airfoils may be determined with about the same accuracy, while the determination of the minimum drag of complete airplane models should be accurate to within 2 per cent or better.

<sup>12</sup> The authors wish to make particular acknowledgment of the courtesy of the Douglas, Boeing, and Northrop Aircraft Companies in permitting the inclusion of the results of such tests as are here discussed.



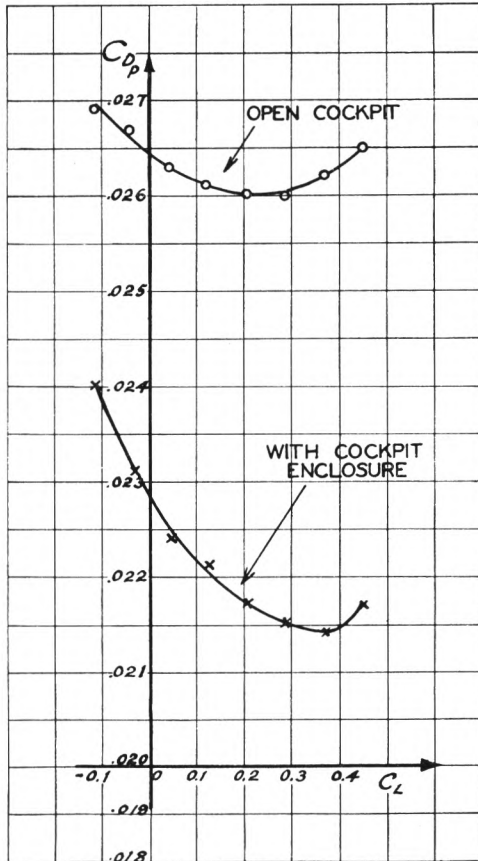


FIG. 11 PARASITE-DRAG COEFFICIENT VERSUS LIFT COEFFICIENT (For complete airplane model with and without cockpit enclosure.)

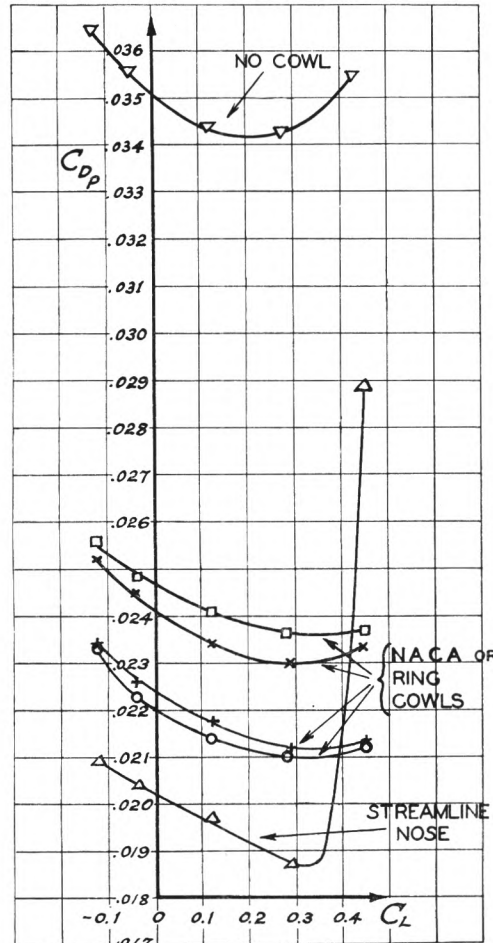


FIG. 12 PARASITE-DRAG COEFFICIENT VERSUS LIFT COEFFICIENT FOR COMPLETE AIRPLANE MODEL (With various radial-engine cowling arrangements. The streamline nose replaced engine and cowl.)

estimated to furnish about 35 per cent of the gross minimum drag of the complete airplane in flying condition. The question as to whether the additional 7 per cent which could be saved by a completely retractable gear is worth the added weight and complication which such a gear entails is one for the designer himself to decide. It might be mentioned that removing the very small fillet which may be seen in Fig. 10 between wing and fuselage caused an increase of 20 per cent over the standard drag.

(b) *Cockpit Enclosures.* In connection with a recent series of tests made for the Boeing Airplane Company, the details of which are still confidential, a model of a very clean airplane was tested with a normal open cockpit with windshield and headrest, and the same model was then tested with a completely streamlined cockpit enclosure. The results given in Fig. 11 furnish a typical example of the very large effects to which such modifications may lead.

(c) *Engine Cowlings.* In connection with the aforementioned tests, the model,

However, if a given model is tested successively with various modifications, the tare drag remains the same for all the tests and the differences in drag between the various model configurations can be determined with much higher accuracy than the foregoing figure. A considerable number of investigations of this type have been made at our laboratory, some of which will be briefly described here.

(a) *Tripod and "Pant Leg" Landing Gears.* A series of measurements was completed in December, 1930, on a model of a Northrop Alpha airplane without engine, cowl, cockpit, or tail surfaces. A normal tripod landing gear and a "pant leg" gear with various modifications were attached. Dimensioned drawings of the landing gears are given in Fig. 9, and a picture of the wind-tunnel model with shortened pant-leg landing gear is given in Fig. 10. The model was tested in the high-speed attitude, the results being obtained at a wind speed of 210 mph. The drag of the model with no landing gear (corresponding to a completely retracted gear) was taken as a standard of comparison, and the percentages of this standard drag added by the various gears are given in Table 1.

Landing gear	Percentages of standard drag added by gear
Pant leg, completely faired	11.0
Pant leg, normal	15.1
Pant leg, shortened	20.0
Tripod	76.2

It will be noticed that the normal pant-leg gear has only one-fifth the drag of the tripod gear, and that the latter would be

which was furnished with a very accurate small-scale reproduction of a standard air-cooled engine, was investigated with a series of four ring- and N.A.C.A.-type cowls. The differences between some of the latter were so slight as to be difficult of detection

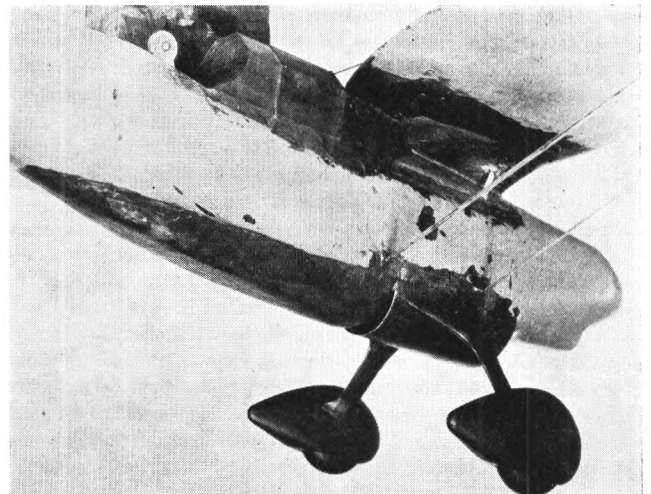


FIG. 13 PHOTOGRAPH OF OPTIMUM COWLING AND STREAMLINING (For "belly" radiator of Douglas YO-31 airplane model.)

upon casual observation. The results given in Fig. 12 show the well-known reduction in drag due to the use of this type of cowl and also furnish evidence as to the possibility of choosing the optimum of a series of very similar configurations, in view of the accuracy indicated by the experimental points.

(d) *Radiator Cowling and Fairing.* In the course of an investigation on a model of a Douglas YO-31 observation plane, it was noticed that a rather large bump placed on the bottom of the fuselage some distance behind the normal "belly" radiator caused no increase in drag. An investigation into the influence of cowlings and fairings in connection with such a radiator was accordingly undertaken. The optimum configuration arrived at is shown in Fig. 13, and the comparative drag measurements showing the results with this configuration and with the standard radiator installation (a short tunnel and no fairing behind) are given in Fig. 14. The precision as indicated by the scatter of the experimental points is again interesting.

(e) *Wing-Engine Nacelles.* A model of a large airplane with two air-cooled wing engines was recently tested in our laboratory wind tunnel. The nacelles and engine cowlings were designed in accordance with the latest recommendations embodied in the exhaustive reports published on the subject by the N.A.C.A. In connection with the particular wing used, it appeared, however, that there were certain undesirable interference effects, especially in the cruising range and near the stall. In the attempt to improve the aerodynamic characteristics, a series of eight modified nacelle-

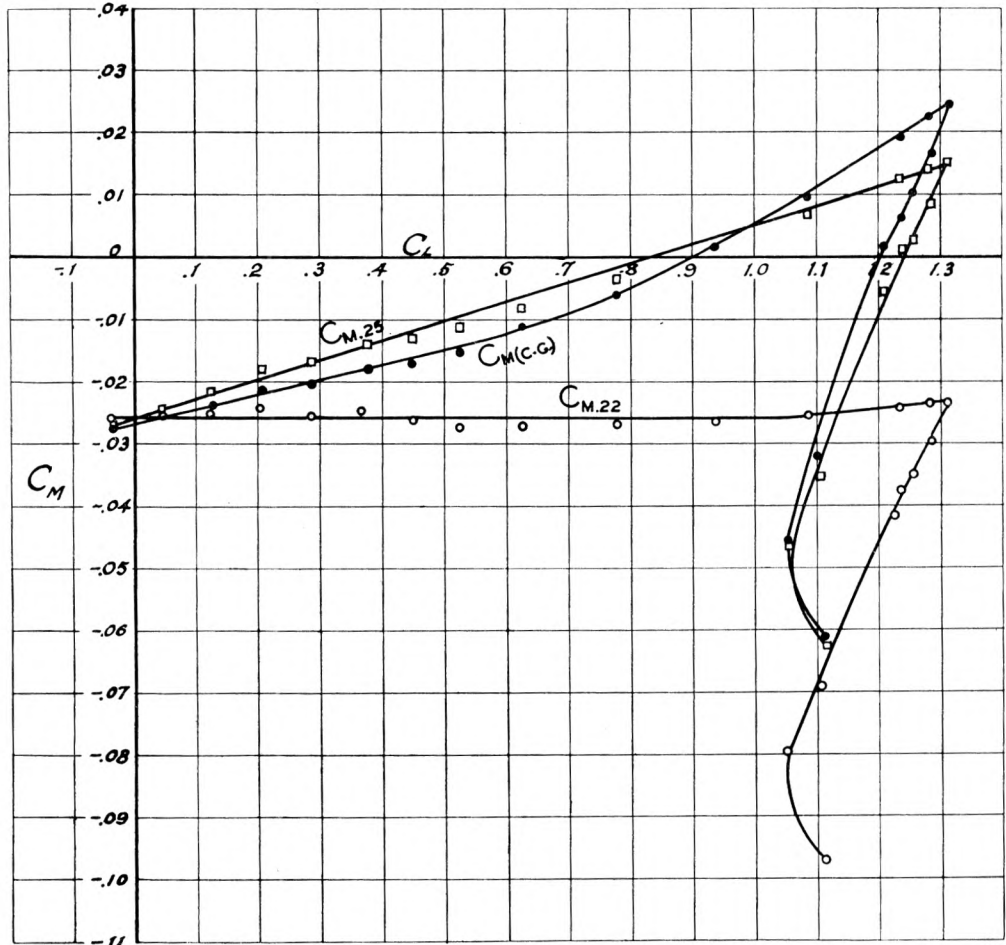


FIG. 15 STALLING-MOMENT COEFFICIENT VERSUS LIFT COEFFICIENT  
(For transport airplane wing only.  $CM_{0.25}$  and  $CM_{0.22}$  give moments about the 25% and 22% points of the calculated mean aerodynamic chord, respectively.  $CM_{C.G.}$  gives moments about the assumed center-of-gravity position of the airplane.)

cowling arrangements and three wing-nacelle fillets was tested. The final or optimum configuration gave, with reference to the original nacelle and cowling as mounted on the model—

- a decrease in minimum parasite-drag coefficient of 0.0006, or 3 per cent of the gross minimum drag;
- a decrease of parasite-drag coefficient in the attitude for single-engined operation of 0.003, or about 10 per cent of the gross drag at this attitude;
- an increase in maximum-lift coefficient of 0.12.

The results of this particular investigation are particularly significant in that they indicate the great value of having one of the designers, who is working on the plane, present and cooperating during the tests. It is very difficult to see how so considerable an aerodynamic improvement, which was structurally and economically entirely feasible, could have been effected if this procedure had not been followed during the investigation.

2 INTERFERENCE PROBLEMS

In this field the most elaborate studies undertaken at our laboratory have been those connected with wing-fuselage interference and reported by A. L. Klein<sup>13</sup> at an aeronautic meeting one year ago. The technique employed in this type of research involves the use of physicist's wax for making alterations to a model, the

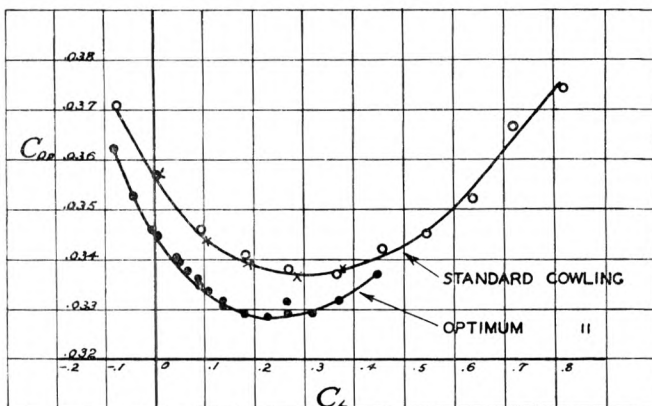


FIG. 14 PARASITE-DRAG COEFFICIENT VERSUS LIFT COEFFICIENT  
(For the configuration of Fig. 13 and for the same model with standard radiator cowling.)

<sup>13</sup> A. L. Klein, "The Effect of Fillets on Wing-Fuselage Interference," presented at Pacific Coast Aeronautics Meeting, June 9 and 10, 1932 (mimeographed).

measurement of lift, drag, and pitching moment on the wind-tunnel balances, and an investigation of the flow pattern behind the model by means of a large number of small pitot and static-pressure tubes connected to a multiple manometer. Since Klein's paper discusses the problem in detail, no further discussion will be attempted here, except the statement that the same technique has been successfully applied in investigating the interference between wings and nacelles, landing gears, protuberances, etc.

### 3 LONGITUDINAL STABILITY AND CONTROL

An interesting example of the contribution which the wind tunnel can make to the problem of static longitudinal stability occurred recently in the course of tests on a model of a large and very carefully designed transport monoplane. The wing had a rectangular center section and considerably tapered outer sections. The mean aerodynamic chord was estimated by the customary methods accepted by present-day designers, and the center-of-gravity location was determined relative to this mean aerodynamic chord so as to give the desired degree of stability. When the complete model was tested, the stability was found to be too small, and when the wing was tested alone, it appeared that the pitching moment coefficient was constant, not about the 25 per cent point of the mean aerodynamic chord, as was to be expected, but about the 22 per cent point. The pitching-moment curves for this wing are shown in Fig. 15. In this case also a designer of the airplane was present at the tests, and a new wing was promptly designed which had the effect of moving the center of gravity of the airplane 3 per cent forward. When the model was retested with this new wing, the stability was almost precisely that expected. In cases which involve more unorthodox than mere wing taper, the contribution which the wind tunnel can make is still more important.

In connection with the recent development of fixed stabilizers

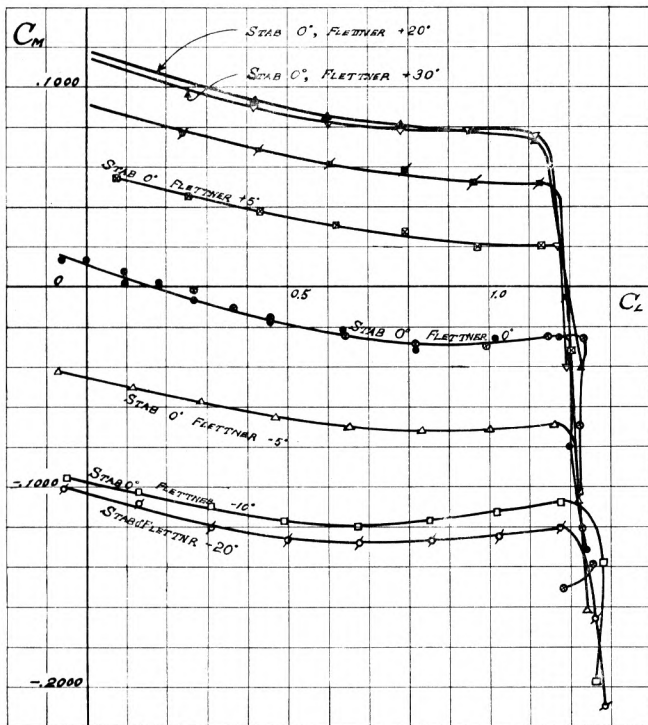


FIG. 16 STALLING-MOMENT COEFFICIENT VERSUS LIFT COEFFICIENT (For model of a complete transport plane with fixed stabilizer, various Flettner angles, and free elevator. The elevator was statically balanced and had ball-bearing hinges.)

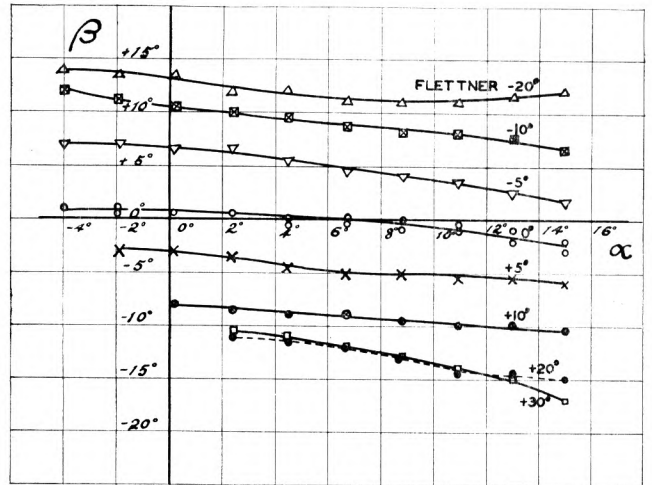


FIG. 17 ELEVATOR ANGLES  $\beta$  FOR VARIOUS FLETTNER SETTINGS [As a function of the angle of attack  $\alpha$  (elevator free). The model was the same as for Fig. 16.]

in which trim is obtained by means of Flettner controls on the elevator, the problems of stabilizer setting, adequacy of elevator control, and effectiveness of the Flettner become extremely important. If the designer is to build the stabilizer as a rigid portion of the fuselage structure, he must know the correct stabilizer setting before building or even designing the plane. This question (at least for power-off flight) can very easily be answered in the wind tunnel, and several such investigations have been made at our laboratory. In order to obtain data with regard to adequacy of elevator control and Flettner effectiveness, the most straightforward procedure is to measure elevator-hinge moments as well as pitching moments for various elevator and Flettner angles. This, however, is a rather awkward and difficult matter on a complete airplane model. The alternative procedure here described has proved very satisfactory. The elevator is attached to the stabilizer by means of very small-size ball bearings which cause no disturbance of the surface of either portion of the tail. Arrangements are also made to clamp elevator and Flettner independently at any desired angle. Runs are first made with Flettner clamped neutral and elevator free, so as to determine the hands-off stability. Then with the model at a series of angles of attack, the Flettner is clamped at various angles and the free-elevator angle is observed. Finally, measurements of the pitching moment are made with the elevator clamped in its extreme positions, both with Flettner neutral and with Flettner setting such that the free elevator assumes its extreme position. These data are sufficient to tell whether or not the plane can be trimmed at any point in the flying range with no force on the elevator controls. A more extensive series of pitching-moment measurements may also be made with elevator free and Flettner clamped at a series of angles. A set of curves of the latter type for an airplane whose controls are ample but whose stability near the stall is not satisfactory are shown in Fig. 16, and a typical family of curves for free-elevator angle at a series of Flettner settings is given in Fig. 17.

### 4 HIGH-LIFT AND AERODYNAMIC BRAKING DEVICES

Several types of high-lift and drag-increasing, or aerodynamic braking, devices have been studied in our laboratory wind tunnel, but of these only one will be discussed here, since it appears at the present time to have considerable advantages over all the others. The bottom surface or split trailing-edge flap was first investigated, as far as the authors are aware, in 1921 in the wind tunnels at McCook Field and the Navy Yard. Unfortunately,



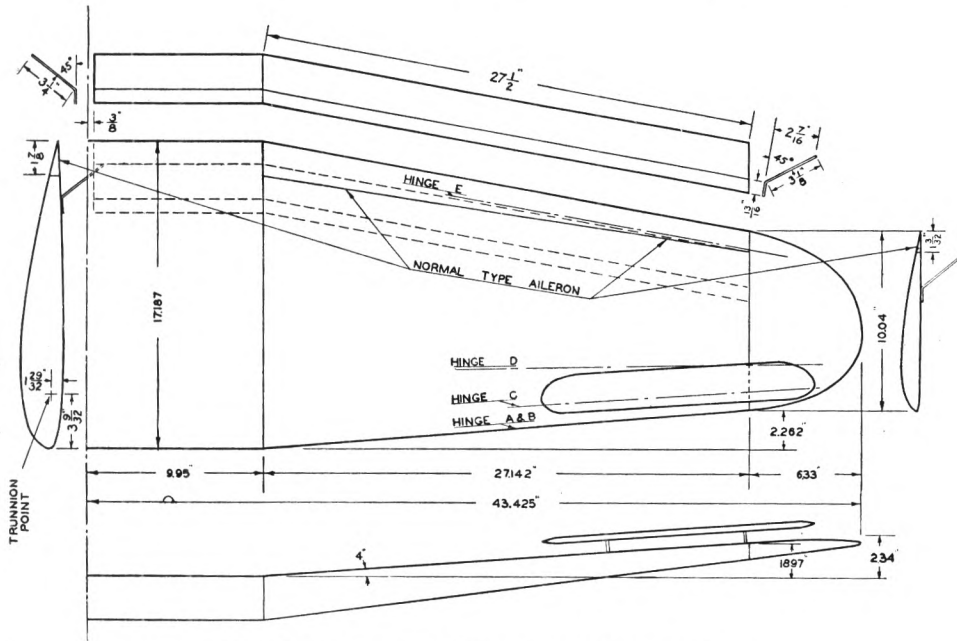


FIG. 18 TAPERED WING WITH BOTTOM SURFACE FLAP  
(Dimensions are in inches and correspond to model scale.)

the reports on these tests have remained confidential and have never been published. A series of tests on a split trailing-edge flap was described by Bamber in 1929.<sup>14</sup> More recently there has been considerable activity in connection with such devices, sponsored to a large extent by the Zap Corporation. Finally, systematic tests dealing with bottom-surface flaps have very recently been made at Göttingen, and an explanation for their effect has been given.<sup>15</sup> In March, 1932, an investigation of an extremely simple type of bottom-surface flap was undertaken for the Northrop Corporation and furnished very interesting results, some of which are here discussed. A paper by Drs. Millikan and Klein describing the experiments and results in detail is appearing currently in one of the technical journals.

The wing used in the tests was a tapered wing whose center section was originally that of the N.A.C.A. 2415, while the tip was 2409. Unfortunately, the wing, which was made of wood, warped considerably during the investigation, so that these sections were not accurate. The wing and flaps are shown in Fig. 18. (The auxiliary airfoil there indicated will be discussed in the next section.) The flap was made of 0.039-in. galvanized iron sheet and was screwed to the bottom of the wing in three sections—one on the center section and one on each outer wing panel. The wing was tested

<sup>14</sup> M. J. Bamber, "Wind-Tunnel Tests on an Airfoil Equipped With a Split Flap and Slot," N.A.C.A. Technical Note No. 324 (1929).

<sup>15</sup> E. Gruschwitz and O. Schrenk, "On a Simple Method of Increasing the Lift of Wings," *Zeits. für Flugtechnik und Motorluftschiffahrt*, vol. 23, no. 20, p. 597 (Oct. 28, 1932).

without flaps, with flap on the center section only, with flaps on the outer wing panels only, and with flaps across both center section and outer wing panels. The results are given in Fig. 19. The curves for flaps and free-air ailerons are discussed in the next section. (It should be mentioned that the curves for the wing without flaps were taken near the end of the investigation, which extended over several months. Similar curves from runs near the beginning of the series of tests did not show the curious flat top at the stall and reached values of  $C_{Lmax}$  of 1.33. It is thought that warping of the model during the investigation caused a twist, so that in the later runs one side of the wing stalled before the other. Slight asymmetries in the flaps might easily counteract this effect, as was apparently the case.) The

increase in  $C_{Lmax}$  from about 1.3 to 2.04 effected by the complete flaps is the most striking feature of the curves. In this connection the effects of center-section and outer-wing flaps appear to be nearly additive. However, the decrease in the  $L/D$  ratio just below the stall from about 13 to about 6 is almost equally noteworthy, since it corresponds to a very considerable increase in the gliding angle for this condition. The increase in the diving moment is rather appalling, and at first sight seems almost to rule out the possibility of using the device practically. However, subsequent tests on a model of a low-wing airplane, with a wing similar to the foregoing, but complete with tail surfaces, eliminate this apparent difficulty. The pitching-moment coefficients for this airplane are shown in Fig. 20 for the configurations without flaps, with outer-wing

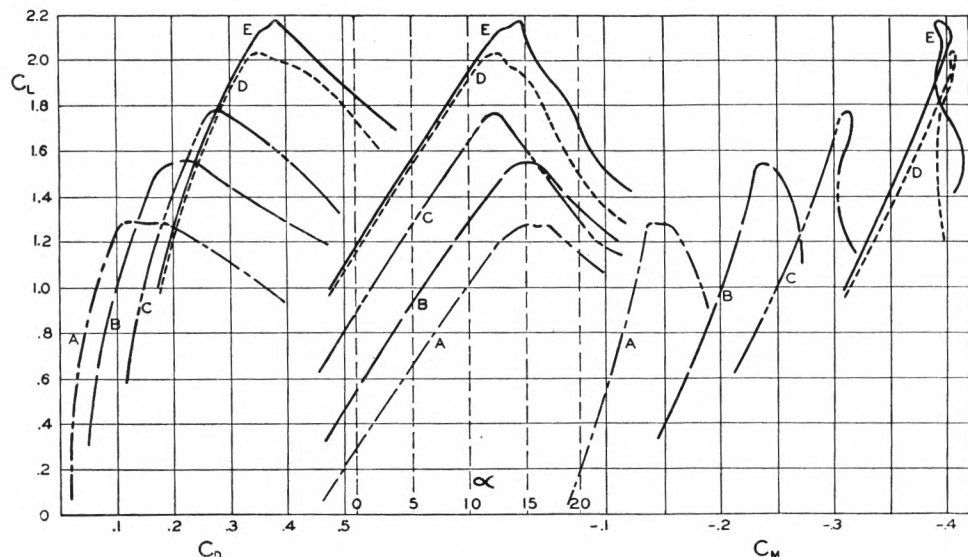


FIG. 19  $C_D$ ,  $\alpha$ ,  $C_M$  VERSUS  $C_L$  FOR THE WING OF FIG. 18

(Stalling-moment coefficients  $C_M$  are referred to an axis through the trunnion point indicated in Fig. 18. The curves refer to the following configurations: A, normal wing, no flaps; B, wing with center-section flap; C, wing with outer-wing flaps; D, wing with complete flaps; E, wing with complete flaps, and free-air ailerons in position A with neutral setting  $-10^\circ$  from reference axis.)

flaps, and with complete flaps. It appears that the addition of the flaps increases the downwash at the tail so much that the large diving moment of Fig. 19 is entirely neutralized for the complete flaps. For the outer-wing flaps the downwash is not quite enough to completely neutralize the flap diving moments, but even in this case the net diving moment produced by lowering the flaps is not unmanageable. In this connection it might be remarked that the Northrop Gamma as built for Frank Hawks and the Ellsworth Antarctic Expedition was equipped with flaps

tion of the problem was undertaken by Klein and Millikan, the detailed results of which appear in the paper to which reference was made in the last section. A brief survey of the most important results is given here.

The two free-air ailerons employed are shown in Fig. 21, and the five locations investigated are indicated in this figure and in Fig. 18 by the hinge locations *A-E*. In Fig. 18 the aileron is shown in position *C*. The wing was also tested with the normal-type ailerons indicated in Fig. 18. Rolling- and yawing-moment

coefficients will be denoted by  $C_r$  and  $C_y$  to avoid confusion, where  $C_r$  = rolling moment/ $qSb$ ,  $C_y$  = yawing moment/ $qSb$ ,  $q$  = dynamic pressure,  $S$  = wing area (not including that of free-air ailerons),  $b$  = wing span. Aileron angles refer to displacements from assumed neutral settings, plus angles corresponding to a lowering of the aileron trailing edge, and minus angles to a raising. The neutral settings are defined by the angle between the reference axes of the aileron and wing as indicated in Fig. 21. The same convention as to signs holds as in the foregoing. The aileron angles are given in pairs, the first figure corresponding to the right aileron and the second to the left. A positive rolling moment is one tending to lower the right wing, and a positive yawing moment is one tending to retard the right wing. It is assumed that if the right aileron is given a negative angle (trailing edge raised), the desirable characteristics are that both rolling and yawing moments are positive. Moments of the desired sign are plotted as full lines, while undesirable signs or reversals of control are plotted as dotted lines. Unfortunately, at the time of these experiments there were not sufficient wind-tunnel balances available to measure lift simultaneously with rolling moment, yawing moment, and side force. Hence the moment curves are plotted against angle of attack uncorrected for wind-tunnel interference ( $\alpha_w$ ), and an auxiliary curve of  $C_L$  versus  $\alpha_w$  is included. This curve is taken from a run with the same wing configuration, but without free-air ailerons. The normal ailerons had a total area of 7.0 per cent of the normal wing area, while the free-air ailerons had 5.6 per cent of the normal wing area.

In Fig. 22 the moments are plotted for the normal ailerons. The yawing moments are unfavorable throughout, and the rolling moments fall off badly at the stall. The relatively small values of  $C_r$  at low lift coefficients are not surprising in view

of the size of the ailerons. Rolling moments for the free-air ailerons in positions *E* and *D* are plotted in Fig. 23. These results are not as accurate as the others presented, since a correction due to side force was not included. However, they show that for the trailing-edge position *E*,  $C_r$  falls off very badly just above the stall, and at *D* the magnitude of the rolling moments up to the stall is unsatisfactory. Position *B* gave results much inferior to *A*, and *C* was likewise not quite as satisfactory as *A*, so that only the latter will be discussed. In Fig. 24, rolling and yawing moments for position *A* without flaps are given, while in Fig. 25 are similar results for position *A* with outer-wing flaps. Several very striking features are apparent.  $C_r$  increases with  $C_L$  up to the stall. This is a very desirable characteristic, since it means that for a given rolling effect the tendency is for the aileron angles to be roughly the same for all angles of attack; i.e., if the control is adequate near the stall, it is not oversensitive at the high-

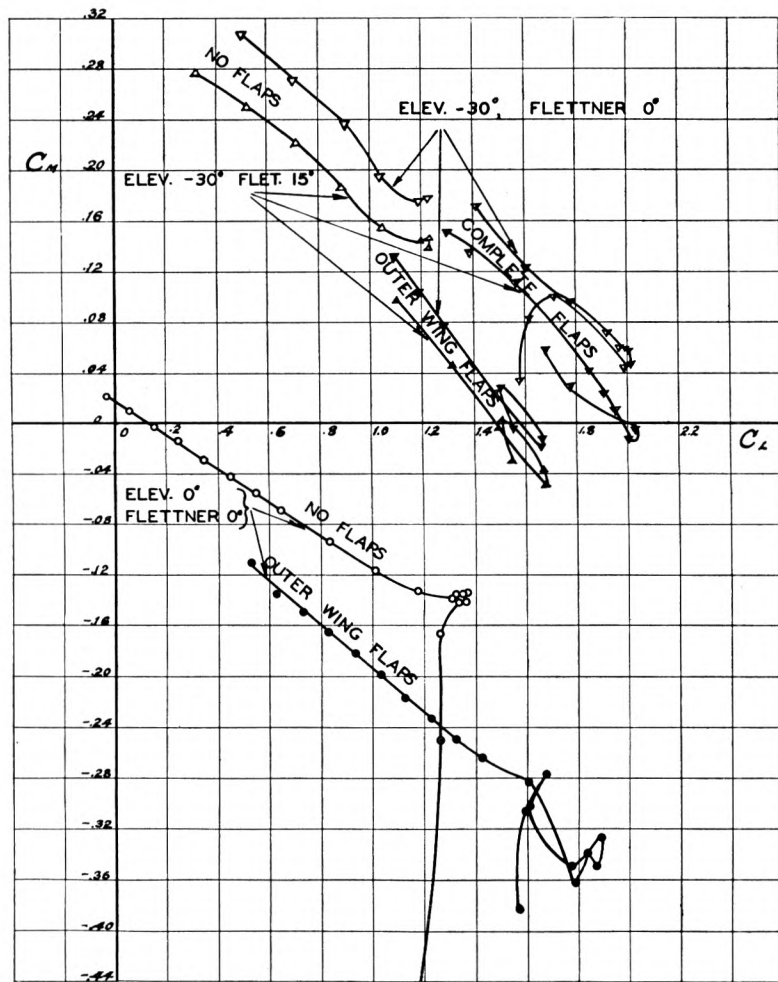


FIG. 20 STALLING-MOMENT COEFFICIENT VERSUS LIFT COEFFICIENT  
(For a low-wing monoplane model with and without bottom surface flaps and with various elevator and Flettner angles.  $C_M$  is referred to the center of gravity of the airplane.)

on the outer wings only, and the lowering of the flaps in flight was accomplished with no difficulties by the pilot.

## 5 LATERAL-CONTROL DEVICES

At the time of the first tests on the bottom-surface flaps attempts were made to secure satisfactory lateral control with the flaps lowered, by various modifications to the normal aileron system. None of these met with success. When the flap mechanism of the Northrop Gamma was designed, there was not sufficient time to permit of wind-tunnel tests on a lateral-control system. Consequently, free-air ailerons were used which were designed in accordance with suggestions from Mr. Temple Joyce. These ailerons were mounted above the trailing edge of the wing. It appeared to the junior author that these ailerons must lose much of their effectiveness at the stall and that a more suitable location should be possible. Accordingly, an extensive investiga-

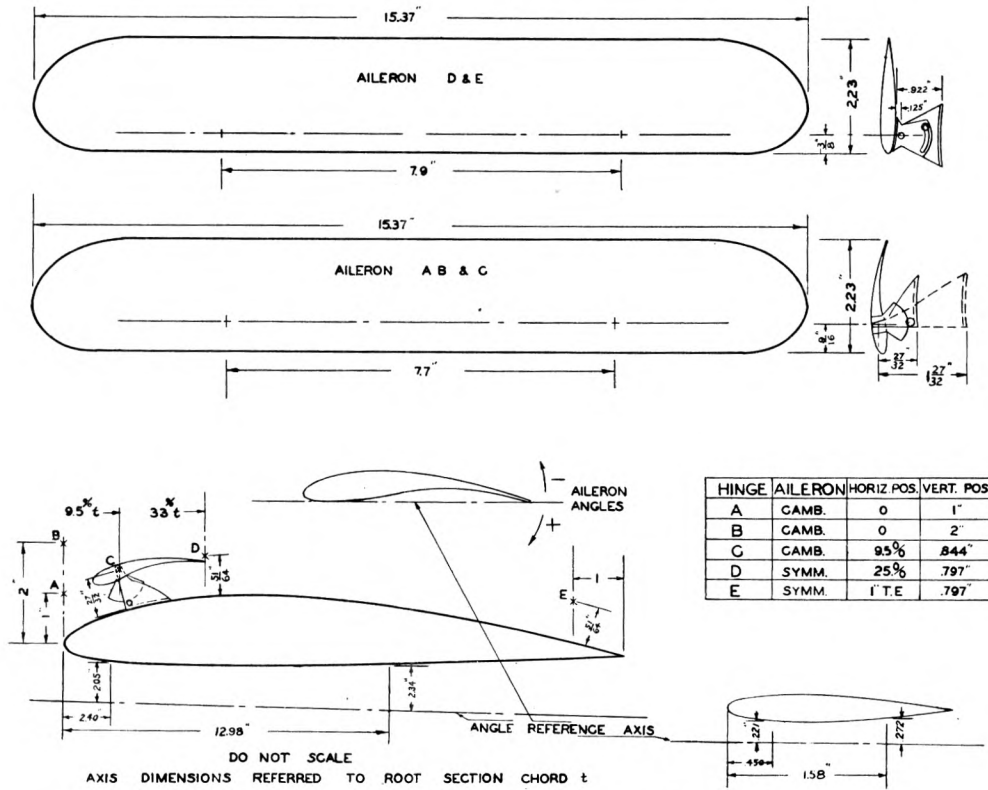


FIG. 21 FREE-AIR AILERON DIMENSIONS AND LOCATIONS  
 (As tested on the wing of Fig. 18. Dimensions are in inches and correspond to model scale.)

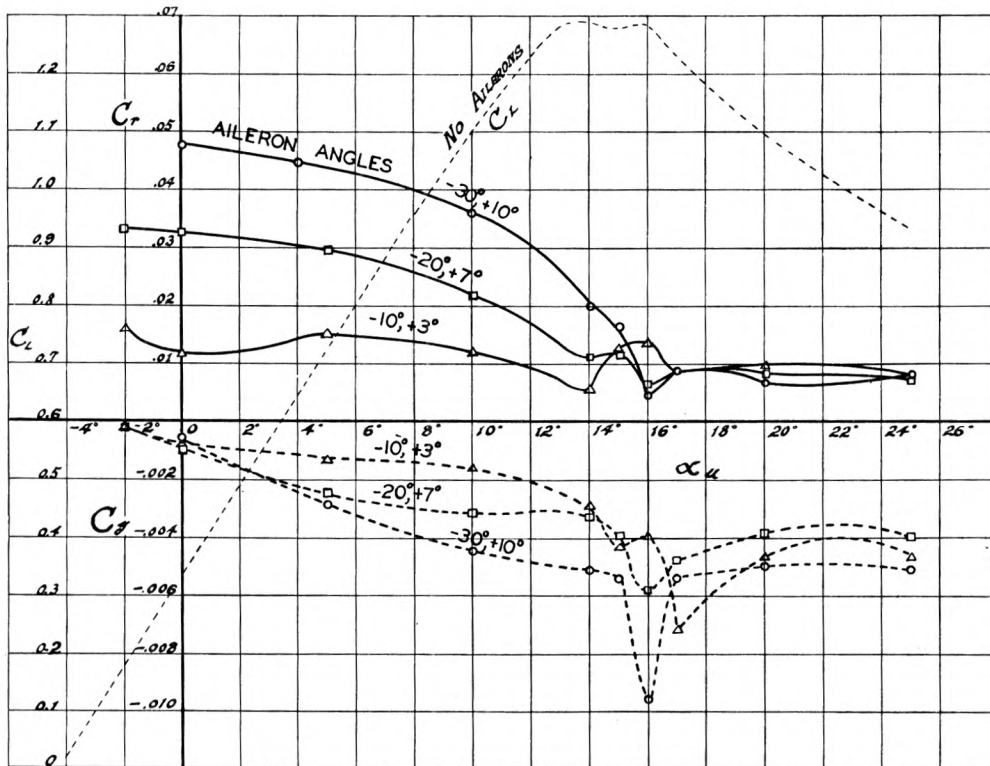


FIG. 22 ROLLING AND YAWING-MOMENT COEFFICIENTS FOR NORMAL AILERONS AT VARIOUS SETTINGS  
 ( $\alpha_u$  is the angle of attack uncorrected for wind-tunnel wall interference. Desirable moments correspond to full lines, undesirable ones to dotted lines.)



speed attitude. The magnitude of  $C_r$  just below the stall is much larger than with the normal ailerons, and a considerable  $C_r$  still remains after the drop above the stall. In this connection it is believed that the oscillations of the curves above the stall are probably due to the lack of symmetry in the wing; i.e., for an accurate and symmetrical wing the curves would probably go approximately through the middle of the waves which appear in the figures. The yawing moments are in the correct sense, except for the cases in which one aileron is at  $4\frac{1}{2}$  deg. This, as well as the negative values of  $C_r$  for  $-6$  deg,  $+4\frac{1}{2}$  deg at

flown in this state. It appears from the results that the most satisfactory linkage for the ailerons would probably be one giving only up travel (i.e., complete differential) and allowing maximum displacements from the neutral setting of about 45 deg. Such a free-aileron system can apparently be designed to give lateral control considerably better than that furnished by most present-day systems, and having the great advantage that its practical effectiveness is not decreased by the use of bottom surface flaps. It should be explicitly pointed out that flight tests on such a free-air aileron system have yet to be reported and

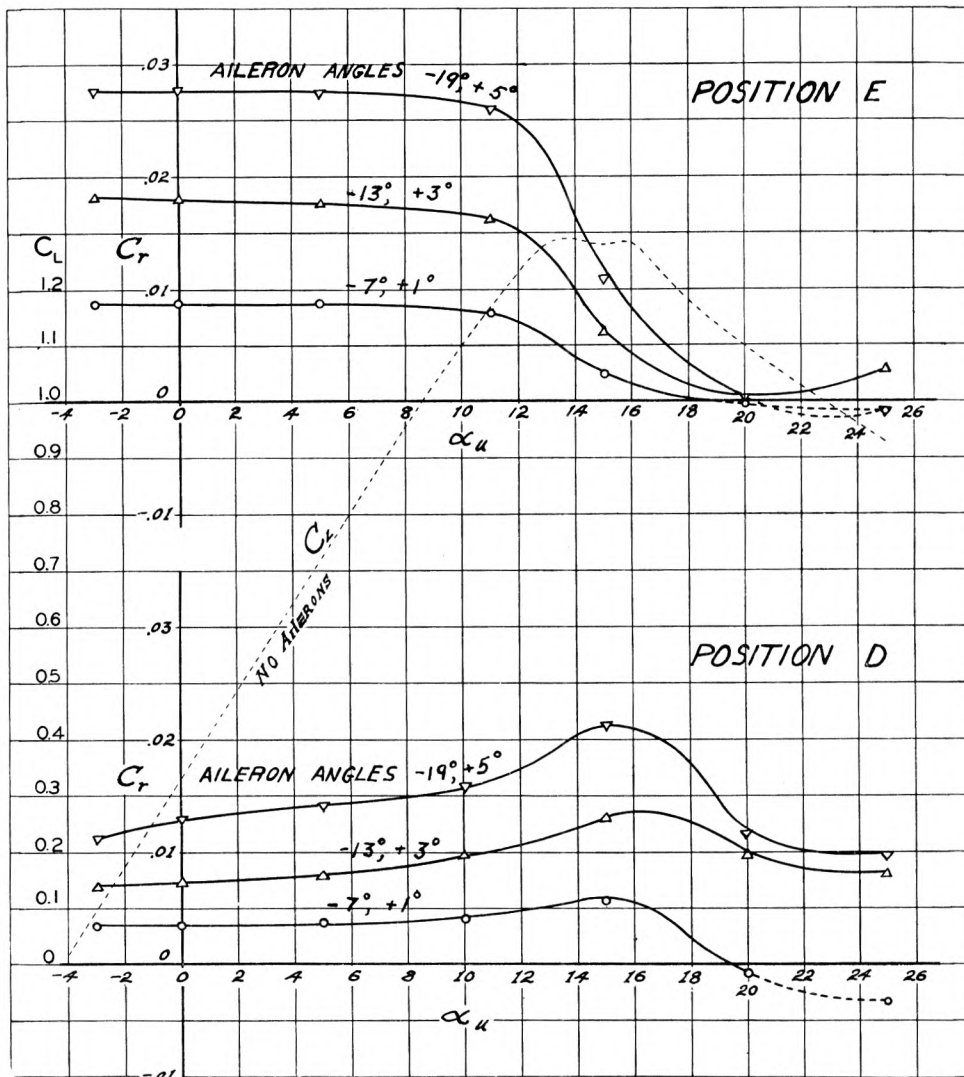


FIG. 23 ROLLING MOMENTS FOR SYMMETRICAL FREE-AIR AILERONS IN POSITIONS D AND E, AT VARIOUS AILERON ANGLES

[The neutral setting in both positions corresponded to aileron angles of  $+1^\circ$  from the wing reference axis (cf. Fig. 21).]

large angles of attack, suggests that for the particular aileron-wing combination employed the optimum arrangement might be one with no down travel of the ailerons. The very large favorable yawing moments for large aileron deflections just below the stall are very satisfactory. The effect of the flaps, at the angles of attack above 5 deg at which they would normally be used, is to increase both rolling and yawing moments for large aileron deflections. The apparent decrease in effectiveness at small angles of attack when the flaps are lowered is probably of no practical importance, since an airplane would almost certainly never be

that the configuration is such that its effectiveness will almost certainly be much affected by minor changes. Hence great caution should be used in the initial attempts to apply the system to an actual airplane.

The effect of the ailerons in position A on  $C_L$ ,  $C_D$ ,  $\alpha$ , and  $C_M$  is shown by the highest curves of Fig. 19.  $C_{Lmax}$  is increased nearly 10 per cent, attaining a value with ailerons and flaps of practically 2.2. The addition to the minimum drag coefficient of the wing only is somewhat less for position A than for any of the others. In the present tests this addition amounts to about

13 per cent of the minimum drag of the wing alone, but a large proportion of this is undoubtedly due to the very crude hinges which were necessary for the wind-tunnel model. The Northrop Gamma was equipped with free-air ailerons in position *E*, which causes more drag than position *A*, and the high performance obtained in flight tests indicates that the overall minimum drag is comparatively small.

6 PRESSURE-DISTRIBUTION MEASUREMENTS

One more field in which the wind tunnel can be of great service to the designer has been brought out by investigations such as those described. Whenever a new device is discovered such as the N.A.C.A. cowl, the bottom surface flap, the free-air aileron, etc., a serious problem arises when the designer attempts to apply it to an actual airplane. For if the device is radically

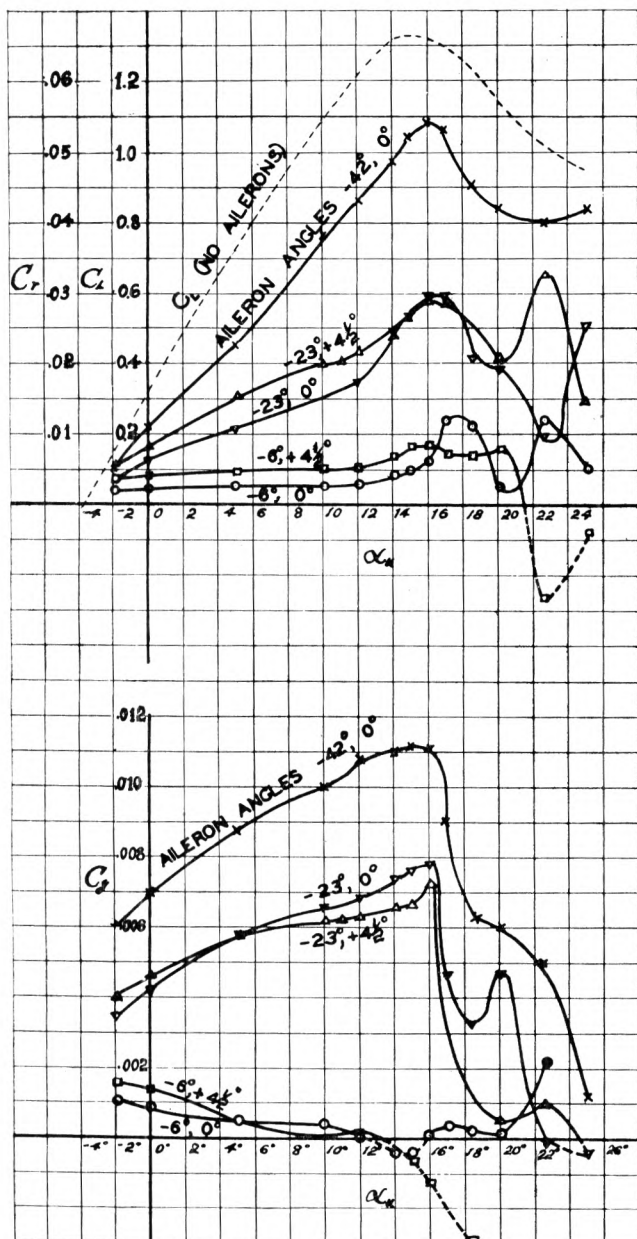


FIG. 24 ROLLING AND YAWING MOMENTS FOR CAMBERED FREE-AIR AILERONS  
(In position *A* without trailing-edge flaps. The neutral setting corresponded to aileron angles of  $-15^\circ$  from the wing-reference axis.)

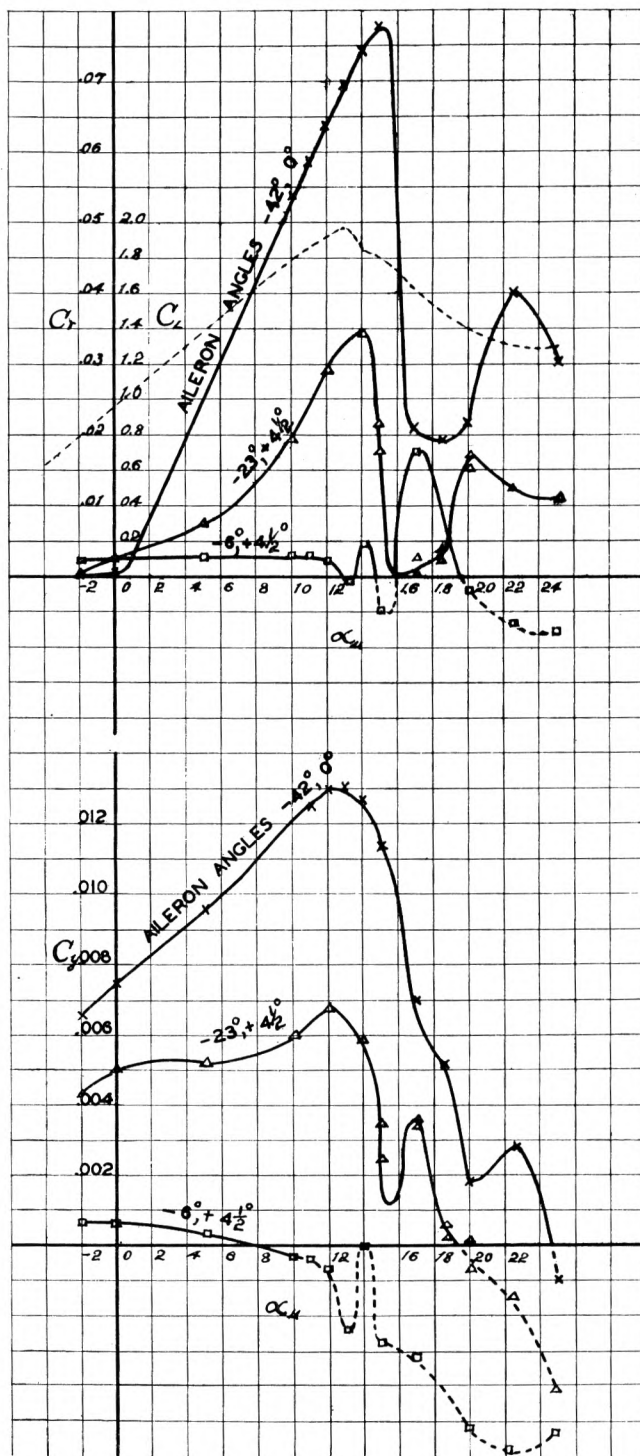


FIG. 25 ROLLING AND YAWING MOMENTS FOR THE CONFIGURATION OF FIG. 24  
(But with bottom surface flaps attached to the outer wing panels.)

new, very few, if any, data exist as to the distribution of forces on which the designer can base his stress analysis. In such cases pressure-distribution measurements are almost essential to obtain the necessary information. Experiments of this nature using a multiple manometer have recently been made at our laboratory on the three devices mentioned and have furnished what are believed to be valuable data for the stress analyst. As long as

new devices are discovered, there will always remain an important field of this character.

#### CONCLUSION

In the first part of this paper a series of general investigations of a more or less scientific nature has been discussed. It possesses in addition to a theoretical interest, a possibility for rather general application to the practical phases of airplane design. In the second part a group of more specialized problems has been considered, all of which originated as investigations of special aspects of particular designs and at the request of airplane manufacturers. The attempt has been made to indicate the varied nature of the problems for which the wind tunnel may

be advantageously used, and the valuable results which may be achieved by close cooperation between the designer and the aerodynamicist conducting the tests have been mentioned. Finally, the way in which such detailed researches often lead to investigations of broad scope and general interest has been illustrated with examples.

[NOTE: Since the paper was presented, the results of the experimental investigation on the effects of turbulence on  $C_{Lmax}$  and of the free-flight measurements of atmospheric turbulence have been published in a paper by C. B. Millikan and A. L. Klein, "The Effect of Turbulence; An Investigation of Maximum Lift Coefficient and Turbulence in Wind Tunnels and in Flight," *Aircraft Engineering*, August, 1933, London.]

---